Transmission electron microscopy study of crystal defects in ZnSe/GaAs(001) epilayers

2000 J. Phys.: Condens. Matter 12 10287

(http://iopscience.iop.org/0953-8984/12/49/330)

J. Phys.: Condens. Matter **12** (2000) 10287–10293. Printed in the UK PII: S0953-8984(00)17524-1

Transmission electron microscopy study of crystal defects in ZnSe/GaAs(001) epilayers

S Lavagne†, C Levade†, G Vanderschaeve†, J Crestou†, E Tournié‡ and J P Faurie‡

† CEMES-CNRS, 29 rue Jeanne Marvig, BP 4347, 31055 Toulouse Cédex, France
‡ CRHEA-CNRS, rue B Gregory, Parc Sophia Antipolis, 06560 Valbonne, France

Received 28 September 2000

Abstract. ZnSe thin films grown on GaAs(001) substrate by molecular beam epitaxy to a thickness of 2500 Å have been studied by transmission electron microscopy (TEM). Three types of structural defect have been observed: (i) Triangle-shaped stacking faults, with the apex close to the interface, either isolated or paired. They are bounded by two different Shockley dislocations. (ii) Stacking faults generated from the surface of the ZnSe epilayer by movement of a Shockley half-loop. (iii) An array of perfect misfit dislocations. Their Burgers vectors are inclined to the interface. Most of them lie along ⟨310⟩ directions; only a few are parallel to ⟨110⟩.

1. Introduction

ZnSe, a wide-band-gap semiconductor ($E_g = 2.80$ eV), is one of the most important materials for the manufacturing of blue-light-emitting devices. However, progress towards the fabrication of efficient devices is still hindered by the short lifetime. The semiconductor performance depends on the distribution and multiplication of the defects during the operation of the device [1]. That is why effort has been focused on the mechanisms of formation of both grown-in defects and degradation defects in heterostructures [2, 3]. Misfit dislocations and triangular stacking faults in pairs or as isolated defects have been studied. However, some controversy remains in the literature regarding the nature of the stacking faults—Frank or Shockley type—and the direction of the misfit dislocations, for instance.

In this work, we report on a transmission electron microscopy (TEM) study of grown-in defects in ZnSe/GaAs(001) heterostructure.

2. Experimental procedure

The (001)-orientated ZnSe/GaAs heterostructure was grown at 280 °C by molecular beam epitaxy in CRHEA Valbonne, France, with an excess of Se [4]. The ZnSe layer was 2500 Å thick (critical thickness $H_c = 1300$ Å); the misfit between the ZnSe and GaAs was 0.27% ($a_{\mathrm{ZnSe}} > a_{\mathrm{GaAs}}$).

Plan-view TEM samples were prepared from the back in the following way: mechanical polishing followed by chemical etching of the GaAs substrate, and finally argon-ion thinning. They were observed using a JEOL 2010 transmission electron microscope operating at 200 kV.

The polarity of the sample was not determined.

0953-8984/00/4910287+07$30.00

3. Results

Four types of defect are observed:

- Misfit dislocations, with a density of about 5×10^4 cm cm^{-2}.
- Half-loops of partial dislocations and triangular stacking faults at a significant density.
- Pairs of triangular stacking faults at a lower density.
- Finally, stacking fault pyramids; these are exceptionally observed.

3.1. Misfit dislocations

An array of long interfacial misfit dislocations is shown in figure 1; some of them are ended by threading segments (T). Most of them (A) lie along unusual ⟨310⟩ directions; a few (B) are along low-energy ⟨110⟩ directions. A-type dislocations have little undulations whereas B ones are very straight. A frequent observation is a sudden change in the line direction, either from ⟨310⟩ to ⟨110⟩ and vice versa or from [110] to $[1\bar{1}0]$ (figure 2). However, changes from [310] to $[3\bar{1}0]$ are never observed.

The Burgers vector is $(a/2)\langle 011\rangle$, which is inclined to the surface.

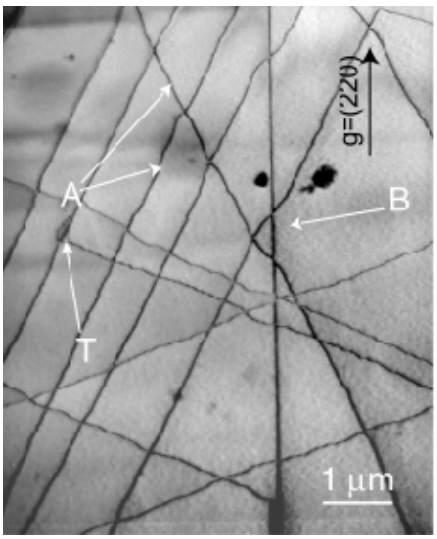

Figure 1. Misfit dislocations. Bright-field image; $g = (220)$; A: ⟨310⟩; B: ⟨110⟩; T: threading dislocation.

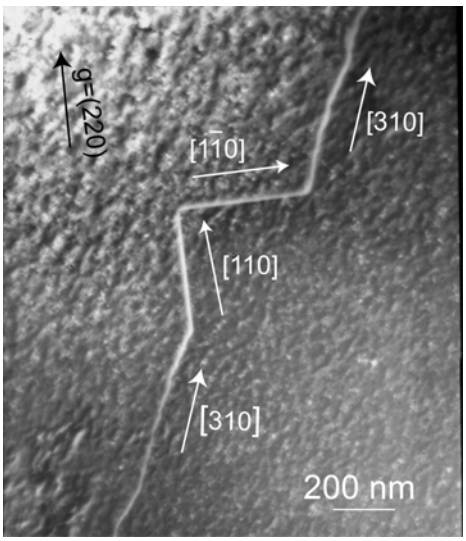

Figure 2. Direction changes of a misfit dislocation. Dark-field image; $g = (220)$.

3.2. Half-loops of partial dislocations

As shown in figure 3, the ZnSe layer contains stacking faults that are limited by a half-loop of a partial dislocation. The dark-field image (figure 3(a)) shows the typical stacking fault contrast. In figure 3(b), only the partial dislocation is in contrast. The Burgers vector is $(a/6)[\bar{1}12]$ in the $(1\bar{1}1)$ plane. Note the disturbed shape of the partial. TEM contrast analysis shows that the stacking fault is extrinsic. It is created by the movement of a Shockley partial, probably nucleated at the sample surface (S). Some of them extend up to the interface (figure 4). This kind of defect lies only in two {111} planes which have the same polarity.

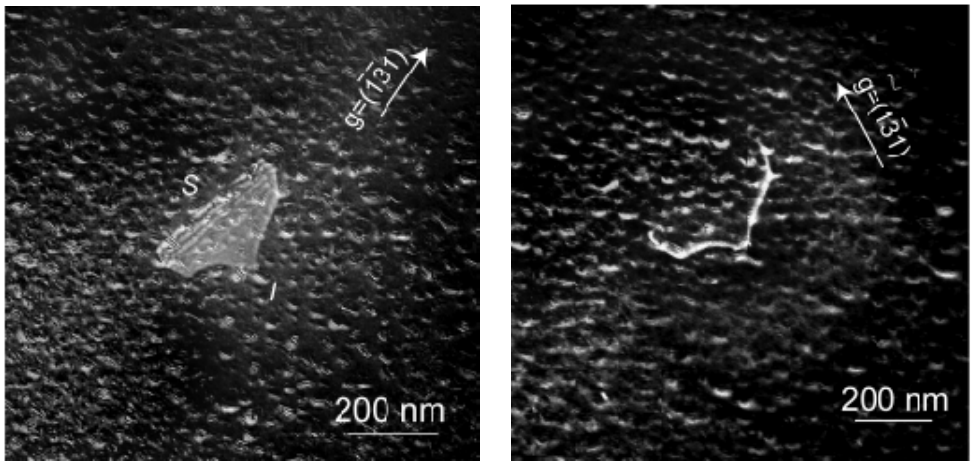

(a) (b)

Figure 3. A half-loop of a partial dislocation in a $(1\bar{1}1)$ plane. (a) Weak-beam dark-field image; $g = (\bar{1}\bar{3}1)$; the fringes are in contrast. (b) Dark-field image; $g = (1\bar{3}1)$; the fringes are invisible and the partial is visible.

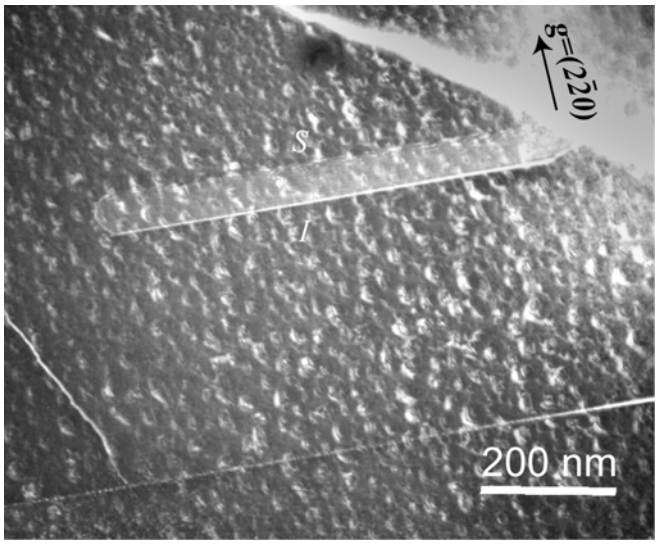

Figure 4. An extended half-loop along the interface; weak-beam dark-field image; $g = (2\bar{2}0)$.

3.3. Isolated triangular faults

Figure 5 shows an example of a second kind of stacking fault: the 'triangular' extrinsic stacking fault, the apex of the triangle being located close to the interface. This fault is bounded by two different 30° Shockley partials that are straight and aligned along ⟨011⟩ directions. This kind of fault is observed only in the same {111} planes as contain half-loops of partial dislocations. Some of them were disappearing during the observation.

In figure 5, the fault plane is $(\bar{1}11)$ and the Burgers vectors are $b_1 = (a/6)[\bar{1}\bar{2}1]$ and $b_2 = (a/6)[1\bar{1}2]$.

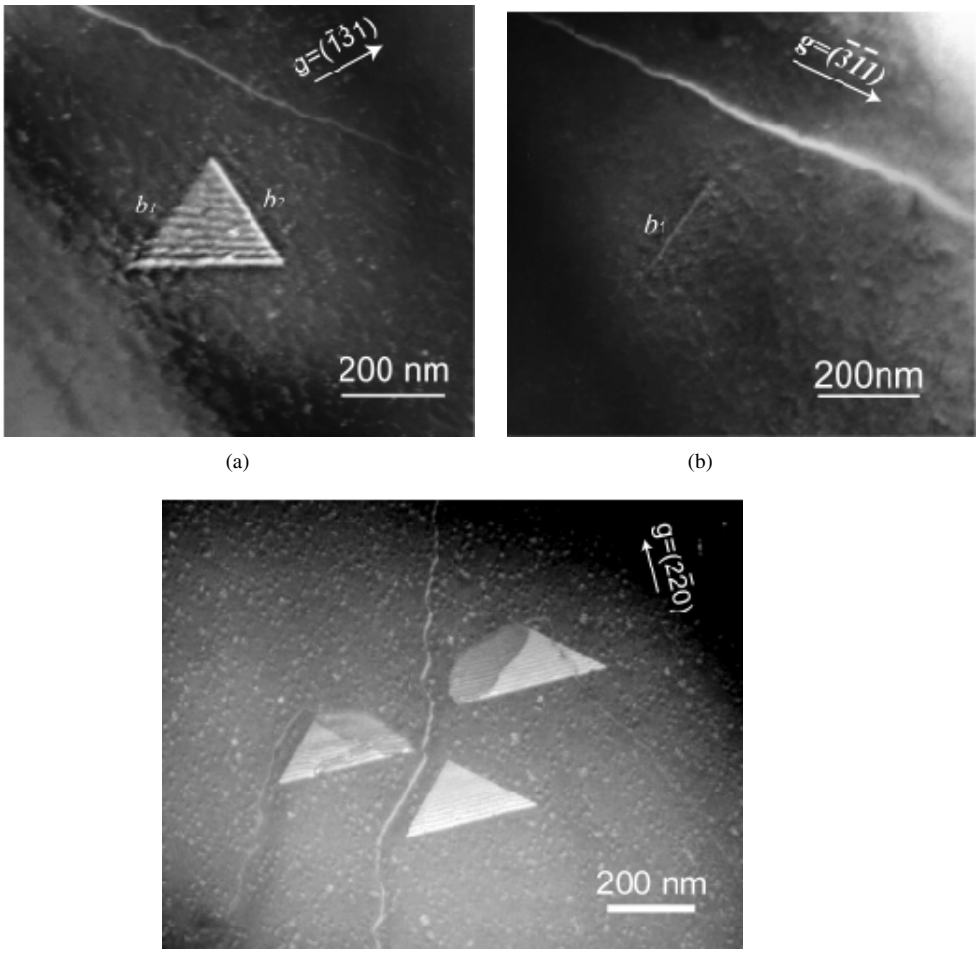

(a) (b)

(c)

Figure 5. Isolated triangular stacking faults in a $(\bar{1}11)$ plane. (a) Weak-beam dark-field image; $g = (\bar{1}\bar{3}1)$; the fringes are visible; the two partials vary in degree of darkness. (b) Weak-beam dark-field image, $g = (\bar{3}\bar{1}1)$; only one partial dislocation is visible. (c) Weak-beam dark-field image; $g = (2\bar{2}0)$; interactions between triangular faults and misfit dislocations.

These triangular stacking faults interact with the misfit dislocations, as shown in figure 5(c). This type of configuration has not yet been fully studied.

3.4. Pairs of triangular faults

Another kind of defect is shown figure 6. These are pairs of intrinsic triangular faults. The pairs lie either in the two {111} planes in zone with [110], or in the two {111} planes in zone with $[1\bar{1}0]$. Each fault is bounded by two Shockley partial dislocations. It can be noted that these partial dislocations have a curved shape, in contrast to the isolated triangular faults. Several extinction conditions have been used to determine the four Burgers vectors; they are indicated in figure 6(c).

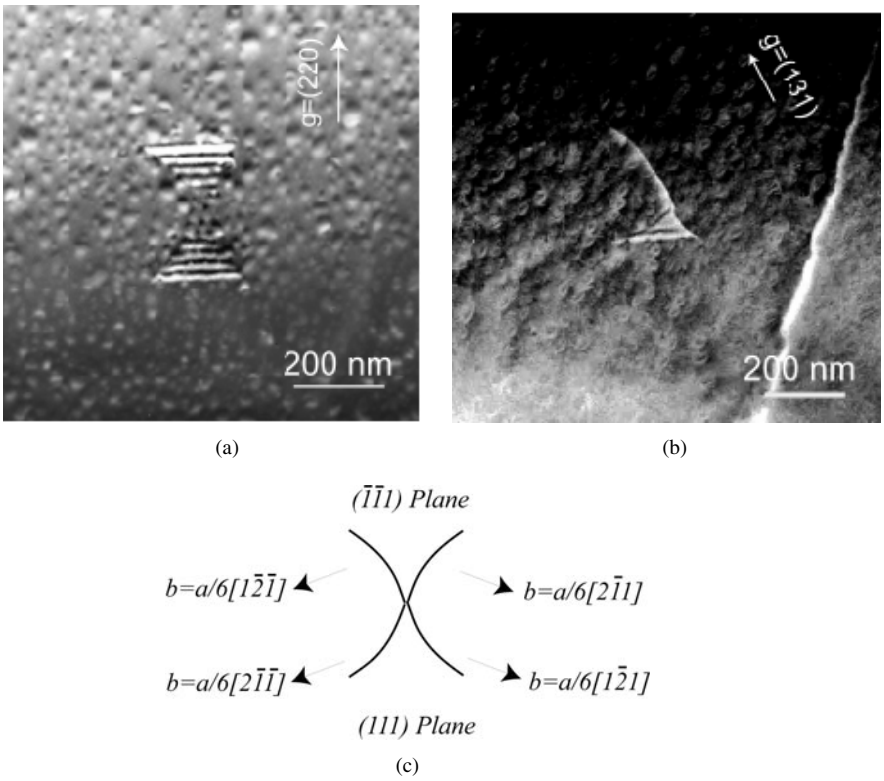

Figure 6. A pair of triangular stacking faults in $(\bar{1}\bar{1}1)$ and (111) planes. (a) Dark-field image; $g = (220)$; the two faults are visible. (b) Weak-beam dark-field image; $g = (131)$; one stacking fault and one partial are invisible. (c) Identification of the Burgers vectors.

4. Discussion

4.1. Misfit dislocations

The misfit dislocations have a Burgers vector which has a component perpendicular to the interface, so they are less efficient as regards plastic relaxation than an array of edge dislocations [5].

Most of the misfit dislocations lie along unusual ⟨310⟩ directions, which are not the lowest-energy line directions in the sphalerite structure. Previous studies have already reported irregular networks consisting of dislocations parallel to the ⟨100⟩ directions in ZnSe heterostructures [6, 7], but to our knowledge, ⟨310⟩ directions have never been observed in this material.

The mean ⟨310⟩ direction could be considered as consisting of short segments lying along the two perpendicular ⟨110⟩ directions of the (001) plane. The weak-beam dark-field images at rather high magnification ($\times 100\,000$) did not allow us to distinguish these short segments. So we may conclude that these segments, if any, should have length less than 3 nm.

Another possibility is that this line direction results from cross-slip in {311} planes, as ⟨310⟩ directions are the traces of those planes in the (001) layer. A similar mechanism has been invoked in an x-ray topography study of GaAs/Ge(001) and $Si_{1-x}Ge_x$/Si(001) strained layers with low lattice mismatch [8]. In that case, the misfit stress can be relaxed by glide

of threading dislocations. When the emergent segment is blocked against an obstacle in a {111} plane, image force and resolved shear stress reduce the dissociation width in this plane and initiate cross-slip in {311} planes. However, the stress level is low in these planes, so the dislocation may rapidly return to {111} planes when meeting a second obstacle. The expected configuration is then along ⟨110⟩ dislocations with some short deviations in ⟨310⟩ directions. Exactly the opposite result is observed here, so we do not believe this mechanism to be efficient in our samples.

4.2. Half-loops of partial dislocations

As we have observed half-loops which have reached the interface, we believe that a glide mechanism is involved in the nucleation of these defects. However, if we consider the fact that the extrinsic fault is bounded by a single Shockley partial, a calculation of the glide force due to the misfit stress leads us to the conclusion that it tends to shrink the stacking fault (equivalently, the component of the Burgers vector in the interface is opposite to what would be expected from the sign of the misfit).

Further work is needed to fully understand the origin of this defect.

4.3. Isolated triangular faults

Contrary to what is found in the literature [9], these faults are not of Frank type. Definite proof is given in figure 5(b). First, it is clearly seen that the fault is limited by two different partials; second, a Frank partial could never have been invisible with a diffraction vector of ⟨311⟩ type. Note that the partials are subjected to a high lattice friction.

4.4. Pairs of triangular faults

These faults are bounded by Shockley partial dislocations, and the curvature of the segment shows that they are different from the previous defects. Similar stacking faults have already been observed in ZnSe heterostructures [10].

This configuration can be interpreted as the result of the intrinsic dissociation of a prismatic half-loop of Burgers vector $(a/2)[1\bar{1}0]$ in the (111) and $(\bar{1}\bar{1}1)$ planes according to the reactions [11]

$$(111): \quad (a/2)[1\bar{1}0] \rightarrow (a/6)[2\bar{1}\bar{1}] + (a/6)[1\bar{2}1]$$
$$(\bar{1}\bar{1}1): \quad (a/2)[1\bar{1}0] \rightarrow (a/6)[2\bar{1}1] + (a/6)[1\bar{2}\bar{1}].$$

5. Conclusions

In this paper, we have characterized the grown-in defects in a 2500 Å thick ZnSe layer on a GaAs substrate. The main results are:

- The misfit dislocations due to strain accommodation have Burgers vectors inclined to the interface and are not parallel to low-energy ⟨110⟩ directions, but rather to ⟨310⟩ directions.
- Numerous stacking faults of different shapes are observed: faulted half-loops and isolated triangular faults which have been characterized as extrinsic faults and pairs of triangular faults which are intrinsic. All of the partial dislocations associated with these stacking faults are Shockley partials.

The mechanisms of formation of these defects are still under discussion.

References

[1] Guha S, Depuydt J M, Qiu J, Haase M A, Wu B J and Cheng H 1994 *Appl. Phys. Lett.* **63** 3023
[2] Kuo L H, Salamanca-Riba L, Depuydt J M, Cheng H and Qiu J 1994 *J. Electron. Mater.* **23** 275
[3] Guha S, Munekata H, LeGoues F K and Chang L L 1992 *Appl. Phys. Lett.* **60** 3220
[4] Bousquet V, Tournié E and Faurie J P 1998 *J. Cryst. Growth* **192** 102
[5] Matthews J 1982 *Dislocations in Solids* vol 2, ed F R N Nabarro (Amsterdam: Elsevier) p 487
[6] Ruvimov S, Bourret E D, Washburn J and Liliental-Weber Z 1996 *Appl. Phys. Lett.* **68** 346
[7] Chen Y, Liu X, Weber E, Bourret E D, Liliental-Weber Z, Haller E E and Washburn J 1994 *Appl. Phys. Lett.* **65** 549
[8] Putero M, Burle N and Pichaud B 2000 *Phil. Mag.* A submitted
[9] Kuo L H and Salamanca-Riba L 1995 *Phil. Mag.* A **71** 883
[10] Bonard J M, Ganière J D, Heun S, Paggel J J, Rubini S, Sorba L and Franciosi A 1997 *Phil. Mag. Lett.* **75** 219
[11] Tanimura J, Wada O and Ogama T 1995 *J. Appl. Phys.* **77** 6223